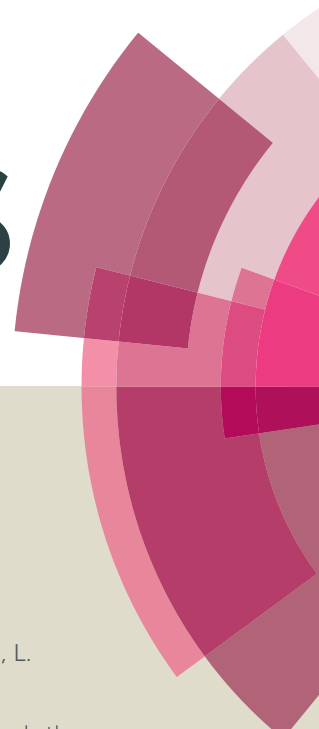


# RSC Advances



This article can be cited before page numbers have been issued, to do this please use: L. Wang, L. Zhu, L. Li and D. Cao, *RSC Adv.*, 2016, DOI: 10.1039/C6RA10073B.



This is an *Accepted Manuscript*, which has been through the Royal Society of Chemistry peer review process and has been accepted for publication.

*Accepted Manuscripts* are published online shortly after acceptance, before technical editing, formatting and proof reading. Using this free service, authors can make their results available to the community, in citable form, before we publish the edited article. This *Accepted Manuscript* will be replaced by the edited, formatted and paginated article as soon as this is available.

You can find more information about *Accepted Manuscripts* in the [Information for Authors](#).

Please note that technical editing may introduce minor changes to the text and/or graphics, which may alter content. The journal's standard [Terms & Conditions](#) and the [Ethical guidelines](#) still apply. In no event shall the Royal Society of Chemistry be held responsible for any errors or omissions in this *Accepted Manuscript* or any consequences arising from the use of any information it contains.

**Tetraphenylethene -functionalized diketopyrrolopyrrole solid state emissive molecules: enhanced emission in the solid state and as a fluorescent probe for cyanide detection**

Lingyun Wang <sup>a\*</sup>, Linhui Zhu <sup>a</sup>, Lin Li <sup>b\*</sup>, Derong Cao <sup>a</sup>

<sup>a</sup> School of Chemistry and Chemical Engineering, State Key Laboratory of Luminescent Materials and Devices, South China University of Technology, Guangzhou, China, 510641

<sup>b</sup> School of Food Science and Engineering, South China University of Technology, Guangzhou, China, 510641

\*Corresponding author: Tel. +86 20 87110245; fax: +86 20 87110245. E-mail: [lingyun@scut.edu.cn](mailto:lingyun@scut.edu.cn); [felinli@scut.edu.cn](mailto:felinli@scut.edu.cn)

## Abstract

Two conjugates of tetraphenylethene (TPE) and diketopyrrolopyrrole (DPP) were synthesized and their fluorescence properties were investigated. Both **DPP1** and **DPP2** show intense fluorescence and large Stokes shifts in both solution and solid state. In dilute THF, **DPP1** and **DPP2** show emission peaks at 606 nm and 632 nm with  $\Phi_f$  32% and 11%, respectively. However, their powder samples for **DPP1** and **DPP2** emit at 650 nm and 615 nm with  $\Phi_f$  13% and 7%, respectively. Moreover, **DPP2** shows remarkable selectivity and specificity toward  $\text{CN}^-$  over other anions. The color changed from pink to colorless when  $\text{CN}^-$  was added to **DPP2** in THF. The maximum emission intensity at 632 nm is quenched 94.6%, which constitutes the fluorescence signature for cyanide detection. The detection limit is 0.3  $\mu\text{M}$  using the fluorescence spectra changes, which is far lower than the WHO guideline of 1.9  $\mu\text{M}$ .

**Keywords**, Chemosensors; Cyanide anion; Tetraphenylethene; Diketopyrrolopyrrole; Aggregation-induced emission (AIE)

## 1. Introduction

As strongly fluorescent heterocyclic pigments, diketopyrrolopyrrole (DPP) and its derivatives have been extensively applied in fluorescent probes,<sup>1</sup> and their structures can be easily optimized through variations of substituents at the 2,5- and 3,6-positions. They exhibit large extinction coefficients, high fluorescence quantum in dilute solution, brilliant red-fluorescence emission and exceptional light, weather, and heat stability. As a consequence of the well-conjugated DPP core, however, they display a typical aggregation-caused quenching (ACQ) effect. It is a great challenge to sustain the efficient emission of DPP-based compounds in aggregated states due to the serious intermolecular  $\pi$ - $\pi$  stacking, making realization of their full potential a daunting task. To overcome this problem, it is a rational strategy to attach bulky or aggregation-induced emission (AIE) substituents onto DPP to hinder the ACQ effect.<sup>2-4</sup> Despite much effort, highly efficient solid emitters based on DPP are very limited.

Tetraphenylethene (TPE) and its derivatives are representatives of AIE active molecules, which possess prominent AIE properties and enjoy the easiness to be synthesized.<sup>5</sup> TPE is also used to modify traditional luminons such as triphenylamine, pyrene, and perylenebisimide and successfully converted them from ACQ to AIE molecules.<sup>6</sup> However, in 2014, Tang's group reported direct linking of TPE to DPP could not convert the DPP derivative from an ACQ to an AIE active molecule and obtained a DPP-based fluorescent material with high quantum efficiency in the solid state.<sup>7</sup> The assimilation of DPP to TPE played a key role. Thus, it is a challenging task

to examine the availability of tuning the emission performance of DPP by rational modifications.

Promoted by the previous report on conjugates of DPP and TPE by Tang's group,<sup>7</sup> we were interested in the further modification of this skeleton to tune its photophysical properties and explore potential applications. It is reasonable that the insertion of a spacer between DPP and TPE moieties may break the assimilation effect. A series of excellent studies have shown that the twisting phenyl ring plays a key role in the organic photo/electronics.<sup>8</sup> Moreover, the double bond is an essential feature for many AIE-active materials and its rigidity in the solid-state prevents the surrounding groups from excessive rotational or vibrational motions.<sup>9</sup> For instance, in our previous work, creation of highly efficient solid emitter by decorating a diphenyl-DPP core with anthracenone by carbon-carbon double bond linker was achieved.<sup>4</sup> Herein, two conjugates containing a diphenyl-DPP core and two TPE arms were synthesized, where the electronic communication between DPP and TPE is crucial for tuning their photo/electronic properties. For **DPP1**, vinyl group, a  $\pi$ -conjugate building block is used as the spacer, which can extend conjugate structure and also induce red-shifted emission. For **DPP2**, an extended  $\pi$ -deficient acrylonitrile spacer was used to blocking the good planarity to optimize its optical properties. The fluorescent behaviors of **DPP1** and **DPP2** in solution and aggregated state were investigated, revealing both dyes with intense fluorescence both in solution and solid state. Due to presence of  $\pi$ -deficient acrylonitrile spacers in **DPP2** and exceptional nucleophilicity of cyanide, **DPP2** can be used as a colorimetric and fluorescent probe for detection of cyanide

ions based on possible nucleophilic addition of  $\text{CN}^-$  to the double bond. **DPP2** showed remarkable selectivity and specificity toward  $\text{CN}^-$  over other anions.

## 2. Experimental

### 2.1. Chemicals and instruments

Nuclear magnetic resonance spectra were recorded on Bruker Avance III 400 MHz and chemical shifts are expressed in ppm using TMS as an internal standard. The UV-vis absorption spectra were recorded using a Helios Alpha UV-Vis scanning spectrophotometer. Fluorescence spectra were obtained with a Hitachi F-4500 FL spectrophotometer with quartz cuvette (path length = 1cm). XRD patterns were collected on a D8 ADVANCE (Bruker).

The absolute fluorescence quantum yield was measured using a Hamamatsu absolute PL quantum yield spectrometer C11347, which consists of an excitation light source based on a xenon arc lamp, an integrating sphere used to measure all luminous flux, and a high-sensitivity multichannel detector. The integrating spheres are generally used to collect the emitted light. The use of integrating spheres has usually required a laser as the excitation source in combination with a fibre coupled CCD camera or a calibrated photodiode as the luminescence detectors. We can fit an integrating sphere into the sample chamber of both the FluoroLog and FluoroMax Spectrofluorometers to measure solid state photoluminescence quantum yields. This approach significantly simplifies the experimental method as the need for special equipment on the excitation and detection side is relaxed.

The THF solutions of anions ( $F^-$ ,  $Cl^-$ ,  $Br^-$ ,  $I^-$ ,  $AcO^-$ ,  $HSO_4^-$ ,  $H_2PO_4^-$ ,  $NO_3^-$ ,  $ClO_4^-$ ) were prepared from their tetrabutylammonium salts.

Benzophenone, phenyl(*p*-tolyl)methanone and (2-bromoethene-1,1,2-triyl)tribenzene were purchased from Sigma. 2,5-Dioctyl-3,6-bis(4'-formylphenyl)pyrrolo[3,4-*c*] pyrrole-1,4-dione (compound **4**) and (2*Z*,2'*Z*)-3,3'-((2,5-dioctyl-3,6-dioxo-2,3,5,6-tetrahydropyrrolo[3,4-*c*]pyrrole-1,4-diyl)bis(4,1-phenylene))bis(2-(4-(1,2,2-triphenylvinyl)phenyl)acrylonitrile) (compound **8**) were synthesized according to our published literature.<sup>4</sup> (2-(*p*-tolyl)ethene-1,1,2-triyl)tribenzene (compound **5**) (2-(4-(bromomethyl)phenyl)ethene-1,1,2-triyl)tribenzene (compound **6**) and 4,4,5,5-tetramethyl-2-(1,2,2-triphenylvinyl)-1,3,2-dioxaborolane (compound **9**) was synthesized according to the literatures reported, respectively.<sup>10-12</sup> The recognition between **DPP2** and different anions was investigated by UV–Vis and fluorescence spectroscopy in THF solution at room temperature. Other solvents were obtained from commercially available resources without further purification.

The stock solution of **DPP2** in THF and anions was at a concentration of 10.0 mM. After the **DPP2** and anions with desired concentrations were mixed, they were measured by UV–Vis and fluorescence spectroscopy.

## 2.2. Synthesis

### 2.2.1 Synthesis of compound **7**

A mixture of compound **6** (650 mg, 1.53 mmol), triphenylphosphine (1.203 g, 4.6 mmol) and DMF (10 mL) were added into a 25 mL round-bottomed flask. The flask was evacuated under vacuum and pushed with dry nitrogen three times. After stirring at 95 °C for 24 h, the solution was cooled to room temperature and poured into large amount of diethyl ether. The 1.030 g white precipitate compound **7** was collected in 98% yield. m.p. 262-263 °C.

<sup>1</sup>H-NMR (CDCl<sub>3</sub>, 400 MHz, δ), 7.79-7.60 (m, 15H, Ph-H), 7.10-6.83 (m, 19H, Ph-H), 5.31 (d, 2H, -CH<sub>2</sub>). <sup>13</sup>C-NMR (CDCl<sub>3</sub>, 100 MHz, δ), 162.5, 144.2, 143.5, 143.0, 142.9, 141.5, 139.8, 135.0, 134.3, 134.2, 131.6, 131.2, 131.1, 130.8, 130.8, 130.1, 130.0, 127.7, 127.6, 127.6, 126.6, 126.6, 126.5, 124.8, 117.9, 117.1, 36.5. HRMS (ESI, m/z), [M-Br]<sup>+</sup> calcd for (C<sub>45</sub>H<sub>36</sub>P), 607.7268, found, 607.7261.

### 2.2.2 Synthesis of compound **DPP1**

A mixture of compound **4** (57 mg, 0.1 mmol), compound **7** (170 mg, 0.3 mmol), K<sub>2</sub>CO<sub>3</sub> (55 mg, 0.4 mmol) and 1,4-dioxane (5 mL) were added into a 25 mL round-bottomed flask. The flask was evacuated under vacuum and flushed with dry nitrogen three times. After 95 °C stirring for 3 h, the solution was cooled to room temperature. The solution was poured into water and extracted with dichloromethane. The organic layer was dried over anhydrous magnesium sulfate. After filtration and solvent evaporation, the residue was purified by column chromatography, using petroleum ether/ dichloromethane/ ethyl acetate (15:5:1 by volume) as eluent. Compound **DPP1** (59 mg) was obtained as a bright red solid in 48% yield. m.p. 238-239 °C.

$^1\text{H-NMR}$  ( $\text{CDCl}_3$ , 400 MHz,  $\delta$ ), 7.84 (d, 4H, Ph-H), 7.61 (d, 4H, olefin H), 7.29 (s, 4H, Ph-H), 7.13-7.05(m, 38H, Ph-H), 3.79(t, 4H, N- $\text{CH}_2$ ), 1.64-1.21 (m, 30H - $\text{CH}_2$ , - $\text{CH}_3$ ).  $^{13}\text{C-NMR}$  ( $\text{CDCl}_3$ , 100 MHz,  $\delta$ ), 162.8, 147.8, 143.9, 143.6, 141.3, 140.4, 140.2, 134.8, 131.8, 131.4, 131.3, 130.6, 129.1, 127.8, 127.7, 127.6, 127.3, 127.0, 126.7, 126.6, 126.5, 126.1, 109.9, 42.1, 31.7, 29.4, 29., 29.0, 26.7, 22.6, 14.0.  $[\text{M}]^+$  calcd. for ( $\text{C}_{90}\text{H}_{84}\text{O}_2$ ), 1225.64, found, 1225.68.

### 2.2.3 Synthesis of compound **DPP2**

A mixture of compound **8** (77 mg, 0.1 mmol), compound **9** (115 mg, 0.3 mmol), and  $\text{Pd}(\text{PPh}_3)_4$  (2 mg) were added into a 100 mL two necked round-bottomed flask. The flask was evacuated under vacuum and flushed with dry nitrogen three times. THF (10 mL) and potassium carbonate solution (2 M, 5 mL) were injected into the flask and the mixture was refluxed overnight. The solution was poured into water and extracted with dichloromethane. The organic layer was dried over anhydrous magnesium sulfate. After filtration and solvent evaporation, the residue was purified by column chromatography, using dichloromethane/ petroleum ether (1.2:1 by volume) as eluent. Compound **DPP2** (37 mg) was obtained as a bright red solid in 29% yield. m.p. 227-228  $^\circ\text{C}$ .

$^1\text{H-NMR}$  ( $\text{CDCl}_3$ , 400 MHz,  $\delta$ ), 8.03 (d, 4H, Ph-H), 7.94 (d, 4H, Ph-H), 7.50 (s, 2H, olefin H), 7.46(d, 4H, Ph-H), 7.14-7.05 (m, 34H, Ph-H), 3.79(t, 4H, N- $\text{CH}_2$ ), 1.62-1.21 (m, 30H, - $\text{CH}_2$ , - $\text{CH}_3$ ).  $^{13}\text{C-NMR}$  ( $\text{CDCl}_3$ , 100 MHz,  $\delta$ ), 161.5, 146.5, 144.5, 142.3, 142.2, 141.2, 138.8, 138.6, 135.2, 131.1, 130.9, 130.3, 130.3, 130.2, 128.6, 128.2, 126.9, 126.8, 126.6, 125.8, 125.7, 124.4, 116.6, 112.1, 109.7, 41.2, 30.7, 28.5,

28.0, 28.0, 25.7, 21.5, 13.04.  $[M + Na]^+$  calcd. for  $(C_{92}H_{82}N_4NaO_2)$ , 1297.644, found, 1297.439.

### 2.3 Computations

Calculations reported in this paper were performed using Gaussian 09 program. Geometry optimizations for **DPP1** and **DPP2** were determined with Becke's three parameter density functional (B3LYP) method using the 6-311G(d, p) basis set. The local minimum for the optimized structure was confirmed through absence of negative frequency.

## 3. Results and discussions

### 3.1 Design and synthesis

The molecular structures of **DPP1** and **DPP2** and their synthetic routes are shown in Scheme 1. Intermediate (compound **4**) was prepared according to the literature.<sup>4</sup> To increase the solubility, the lactam groups were alkylated upon reaction with 1-bromooctane. **DPP1** was prepared by Wittig reaction between compound **4** and TPE-based ylide (compound **7**). To introduce  $\pi$ -deficient acrylonitrile spacer, compound **4** reacted with *para*-bromobenzylcyanide to yield compound **8**. **DPP2** was prepared by Suzuki coupling reaction between compound **8** and 1,2,2-triphenylethene boronic ester (compound **9**). The purity of the resultants and intermediates has been confirmed by NMR spectroscopy and MS spectrometry (Figures S1–S9, Supporting Information). Due to the N-modified octyl chain, **DPP1**

and **DPP2** have good solubility in common organic solvents. This allows their electronic structures to be evaluated with optical absorption, fluorescent emission measurements in solution such as THF, chloroform (CHCl<sub>3</sub>), however, they display poor solubility in hexane and polar solvents such as methanol and water.

### 3.2 Photophysical properties of **DPP1** and **DPP2** in solution and solid state

In THF, the maximum absorption band of **DPP2** at 526 nm shows a red shift of 13 nm compared to that of **DPP1** (513 nm) due to the electron-withdrawing cyano groups of **DPP2**, which is typical for the S<sub>0</sub>-S<sub>1</sub> transition of DPP chromophore (Fig. S10a, Supporting Information). The second absorption band (300–400 nm) for **DPP1** and **DPP2** with peak maximum at 355 and 340 nm, respectively, is due to a  $\pi$ - $\pi^*$  transition involving both the DPP and TPE units. In the fluorescent spectra, the maximum emission wavelength of **DPP2** is observed at 632 nm, which is 26 nm longer than that of **DPP1** (Fig. S10b, Supporting Information). It is interestingly found that both **DPP1** and **DPP2** exhibit a large Stokes shift even up to 100 nm. The results demonstrate that the electron-donating TPE substituent introduced to the DPP core by different spacer affects the electronic structure of **DPP1** and **DPP2**.

The emission study of **DPP1** in different solvents indicates that the luminescent properties are slightly affected by solvent polarity (Fig. S11, Supporting Information). The emission band has no obvious red-shift, but its intensity is reduced with an increase in the solvent polarity. The FL spectra of **DPP2** show similar features as compared to that of **DPP1** in different solvents (Fig. S12, Supporting Information).

The property that we are most interested in is their fluorescent behaviors in aggregated states. So, we investigated the fluorescent behaviors of **DPP1** and **DPP2** in  $\text{CHCl}_3$ /hexane,  $\text{CHCl}_3$ /methanol and THF/water with different volume percentage of hexane ( $f_h$ ), methanol ( $f_m$ ), and water ( $f_w$ ), respectively. Typically, Fig. 1a shows the FL spectra of **DPP1** in  $\text{CHCl}_3$ /hexane. In  $\text{CHCl}_3$ , **DPP1** emits orange fluorescence ( $\lambda_{\text{em}} = 605 \text{ nm}$ ) and the quantum efficiency ( $\Phi_f$ ) is 33%. With increase of  $f_h$ , the strong emission of orange characteristic band is gradually enhanced.  $\Phi_f$  is 44% at  $f_h$  of 90% (Fig. 1b). Besides the increase in PL intensity, the emission peak showed slightly blue-shift from 605 nm to 602 nm with the increase of  $f_h$  from 0 to 90%. The emission photographs of **DPP1** in  $\text{CHCl}_3$ /hexane mixtures with different  $f_h$  values are shown in Fig. 1c. Different fluorescence effect of **DPP1** in  $\text{CHCl}_3$ /methanol mixtures is present (Fig. 2). When  $f_m < 40\%$ , the emission intensity monotonously increases to negligible. When  $f_m > 40\%$ , aggregates form in the system and the emission intensity greatly decreases. The  $\Phi_f$  is only 9% at  $f_m$  of 90%.

As demonstrated by the FL spectra in Fig. 3, in THF solution, **DPP1** emits orange fluorescence ( $\lambda_{\text{em}} = 605 \text{ nm}$ ) with  $\Phi_f$  of 32%. When relative low fraction of water ( $f_w$ , by volume, 40%), a non-solvent to **DPP1**, is introduced into the THF solution, slightly enhancement in emission intensity is present. When  $f_w$  reaches 50%, the emission intensity decreases greatly. The change in fluorescence intensity vs.  $f_w$  is shown in Fig. 3b. The  $\Phi_f$  is only 3% at  $f_w$  of 90%. The decrease of quantum efficiency against the increase of  $f_w$  can be ascribed to the formation of aggregates in the THF–water mixtures, which quenches the fluorescence *via* the intermolecular  $\pi$ – $\pi$

interaction. Besides the decrease in emission intensity, the emission peak red-shifted from 605 to 619 nm with the increase of  $f_w$  from 0 to 90%. Such an observation clearly indicates that the hydrophobic **DPP1** molecules had formed large aggregates, as both water/THF are hydrophilic solvents and only those smaller ones in the suspension contributed to the emission. To understand mode of aggregation, we have performed UV-vis absorption spectra of **DPP1** in THF/water (Fig. S13, Supporting Information). Aggregation effect in which a reduction in the peak intensity and significant red-shift of the absorption maximum along with loss of fine structure are seen in THF/water as compared to bands in THF alone. The absorption tails extending well into the long wavelength region indicate that **DPP1** aggregate into particles in the presence of water, as it is well known that the Mie effect of nanoparticles can cause such level-off tails in the absorption spectra.<sup>13</sup>

The PL spectra of **DPP2** clearly show similar features as compared to that of **DPP1** in different solvent mixtures. As shown in Fig. S14 (Supporting Information), the emission of **DPP2** in the  $\text{CHCl}_3$  solution is strong with an emission maximum at 628 nm ( $\Phi_f = 15\%$ ). When hexane, a non-polar and poor solvent to **DPP2**, is introduced into the  $\text{CHCl}_3$  solution, the PL signal is gradually enhanced upon increasing hexane/ $\text{CHCl}_3$  ratios. When  $f_h$  reaches 80%, the PL intensity is boosted to the maximum. The quantum efficiency of **DPP2** is 1.3-fold higher than its original emission intensity in  $\text{CHCl}_3$ . However, the emission intensity monotonously decreases when polar and poor solvent of methanol is added to  $\text{CHCl}_3$  solution (Fig. S15, Supporting Information). The  $\Phi_f$  is only 4% at  $f_m$  of 90%. It is noted that the emission peak gradually blue-shifts

from 628 to 624 nm when  $f_m$  is increased from 0 to 90%. Such a spectral shift can be explained as follows: with increased methanol content, **DPP2** molecules start to aggregate, which generates less polar microenvironment for the molecules inside the aggregates. The reduced environment polarity leads to the observed blue shift in the emission spectrum.<sup>14</sup> The similar behavior was also observed for THF/water mixtures, only 4%  $\Phi_f$  was shown in presence of 90% water (Fig. S16, Supporting Information).

Usually, emission of DPP derivatives is never observed in the solid state, because the emission is completely quenched by  $\pi$ - $\pi$  interaction in aggregation. As expected, no emission was observed for pure compound **4** as shown in Fig. S17 (Supporting Information). It is intriguing to note that **DPP1** and **DPP2** still retain intense fluorescence even in the powder form. This observation prompted us to investigate their photophysical properties in the solid state in details. The emission spectra, together with photographs taken under UV illumination, are shown in Fig. 4. Upon exciting at 365 nm, **DPP1** in powder emits strongly in the red region. With respect to corresponding emission at 606 nm in THF solution, the fluorescence maxima peak at 650 nm for **DPP1** in powder is obviously red-shifted. However, it is quite surprising that the emission maximum of **DPP2** in powder is located at 615 nm, which is hypochromic shift of 17 nm than that in THF. This indicates that the **DPP2** fluorophores are still in their isolated form in the powder without heavy intermolecular interactions, as strong  $\pi$ - $\pi$  overlaps in the aggregated or solid state always causes delocalization of the excited states and induces emission at a longer wavelength.<sup>15</sup> However, this is not true for **DPP1**. Evidently, the highly distorted and

rigidified conformation of the TPE unit in **DPP1** and **DPP2** may lead to an extended  $\pi$ - $\pi$  interplanar distance and/or inefficient  $\pi$ - $\pi$  overlap when molecules are aggregated.

The fluorescence quantum efficiency ( $\Phi_F$ ) of the samples was estimated using Rhodamine 6G ( $\Phi_F=95\%$  in ethanol) as standard solution and  $\Phi_F$  of the solid film was measured using an integrating-sphere photometer. **DPP1** ( $10^{-5}$  M) in cast film shows a fluorescence quantum yield ( $\Phi_F$ ) 13%, which is lower than its  $\Phi_F$  in  $\text{CHCl}_3$  and THF *i.e.* 33%, 32% respectively. Interestingly, **DPP2** shows quite different behavior than **DPP1**. It is found that the  $\Phi_F$  of **DPP2** in cast film is 7%, which is lower than  $\Phi_F$  in  $\text{CHCl}_3$  and THF is 15%, 11%, respectively. However,  $\Phi_F$  of **DPP1** and **DPP2** in solid state are higher than that of DPP-triphenylamine dyes ( $\Phi_F=0.03\%$ , 0.1%),<sup>3b</sup> DPP-TPE dye with donor-acceptor effect ( $\Phi_F=8.6\%$ )<sup>7</sup> and others.<sup>16</sup> It should be noted that the introduction of phenylacrylonitrile leads to a larger Stokes shift but a lower  $\Phi_F$  both in solution and solid-state as compared with **DPP1**. The corresponding photophysical data are shown in Table 1.

The morphology of **DPP1** and **DPP2** powders were further investigated by X-ray diffraction (XRD), which show many sharp and strong peaks, indicative of their crystalline nature (Fig. 5). In our case, the molecules of **DPP1** and **DPP2** may steadily cluster together to form ordered microstructures and hard to be changed due to the restriction of the crystal lattice, and this may make the crystals stronger emitters because of the weakened  $\pi$ - $\pi$  interactions among the fluorophores. These results will provide the way to tune the performance of organic luminogens by making subtle

balance between AIE and ACQ units; and on the other hand, derived red-emitting molecules with good quantum efficiency.

### 3.3 Theoretical calculations

The red-shift of emission of **DPP1** and **DPP2** relative to compound **4** (DPP-aldehyde in THF,  $\lambda_{ab} = 497$  nm,  $\lambda_{em} = 592$  nm) is associated with the segmental electronic conjugation between DPP and TPE moieties, as predicted by theoretical calculation (Fig. S18, Supporting Information). In the free state of **DPP1**, the dihedral angle between the vinyl bridge and the adjacent phenyl in the TPE moiety is about  $2.966^\circ$ , suggesting the good conjugation between the TPE and DPP moieties. In comparison with **DPP1**, the large dihedral angle between the acrylonitrile bridge and the adjacent phenyl in the TPE moiety is  $26.739^\circ$  for **DPP2**. Moreover, the dihedral angles between the vinyl bridge and adjacent another phenyl adjacent to DPP core are  $4.174^\circ$  and  $9.637^\circ$  for **DPP1** and **DPP2**, respectively. These results indicate that the addition of the acrylonitrile groups between DPP and two TPE moieties reduces planarity of **DPP2**.

To further elucidate the effect of the spacer on the electronic structures and thus the photophysical properties of the DPP dyes, we conducted total energy calculation using density functional theory (DFT) calculations at the B3LYP/631G(d) level of theory. The density maps of their molecular orbitals are shown in Fig. 6, and the calculated data are summarized in Table 1. **DPP1** has a HOMO delocalized over the vinylbenzene moiety and the entire TPE arms, whereas its LUMO is mostly localized

on the central DPP and vinylbenzene moieties. The HOMO and LUMO energy levels are -5.17 eV and -1.69 eV, respectively. It is noteworthy that in sharp contrast to the remarkable contribution of vinylbenzene moiety to the LUMO for **DPP1**, **DPP2** has a HOMO delocalized over the entire TPE arms, whereas its LUMO is mostly localized on the central DPP, benzene and acrylonitrile moieties. The HOMO and LUMO energy levels are -5.38 eV and -2.21 eV, respectively. The decreased HOMO–LUMO gap of **DPP2** should be responsible for the red-shifted main emissive band relative to that of **DPP1**. All the calculated results are in good agreement with the experimental results.

#### 3.4. Detection of cyanide with **DPP2**

Cyanide has been continuously of concern all over the world due to its high toxicity and widespread use in industrial processes such as acrylic fiber manufacturing, metallurgy, herbicide production, and silver or gold extraction.<sup>17</sup> Therefore, it is of great significance to find convenient and efficient detection methods at the environmental and biological levels. The burgeoning field of reaction-based indicators has made progress in this area because of the unique reactivity of  $\text{CN}^-$  toward a variety of organic functional groups including C=O, C=N, C=C, and so on.<sup>18</sup> The irreversible formation of chemical bonds can provide chemodosimetric information and develop ratiometric fluorescent probes. It is well known that general Michael acceptors, the doubly activated acceptors, in which two electron-withdrawing groups are attached to the C=C group, are more reactive, and allow the Michael addition

reaction to occur under mild condition. Clearly, to improve the sensitivity, it is necessary to enhance the reactivity of the probe to cyanide. With this in mind, we recently reported chemodosimeter approaches based on diketopyrrolopyrrole, where electron withdrawing cyano and ester groups or 1,3-indanedione to afford doubly activated Michael addition type probes for the colorimetric fluorescent detection of cyanide with high sensitivity and good selectivity.<sup>19</sup>

The interaction of **DPP1** in THF with cyanide through absorption and fluorescence spectra titration experiments was carried out. As shown in Figs. S19-S20 (Supporting Information), no changes could be found in presence of cyanide. **DPP1** is inactive to cyanide due to low reactivity of vinyl group in **DPP1**. However, **DPP2** may have great potential for detection of cyanide due to presence of  $\pi$ -deficient phenylacrylonitrile section, electron withdrawing cyano group connected with the  $\alpha$ -position of the ethylenic bond. The interaction of **DPP2** in THF with cyanide through absorption and fluorescence spectra titration experiments was carried out. **DPP2** exhibits main absorption bands centered at 336 and 525 nm, respectively (Fig. 7). Upon addition of 0–24.0 equiv. of cyanide, both bands gradually decrease and the one at 525 nm eventually vanishes at the saturation point (24.0 equiv.). Two new bands at 312 nm and 360 nm are present. This change suggests that the large  $\pi$ -conjugation is interrupted, accompanied by the formation of  $[\mathbf{DPP2-CN}]^{2-}$  due to the nucleophilic attack of cyanide toward the acrylonitrile groups of **DPP2**. Moreover, the solution faded and became almost colorless, which could be clearly observed by naked eye (Fig. 7 inset).

As expected, the fluorescence emission of **DPP2** is quenched by the nucleophilic addition reaction between cyanide and acrylonitrile group. Upon excitation at 520 nm, a broadened emission band at around 632 nm is detected, which gradually decreases upon addition of cyanide and became saturated with 52.0 equiv. of  $\text{CN}^-$  (Fig. 8). Finally, 94.6% PL intensity at 632 nm is quenched. Additionally, a linear relationship between the fluorescent intensity at 632 nm and the concentration of  $\text{CN}^-$  in the low concentration region is obtained (Fig. S21, Supporting Information). The detection limit is as low as 0.3  $\mu\text{M}$ , which is much lower than the maximum contaminant level for  $\text{CN}^-$  in drinking water (1.9  $\mu\text{M}$ ) set by the World Health Organization (WHO).<sup>20</sup> In comparison with reported probes,<sup>21</sup> the detection limit of **DPP2** is moderate for fluorescence detection limits to cyanide.

For the purpose of evaluating selectivity of **DPP2** to cyanide, the absorption spectral change of **DPP2** upon addition of other anions was also investigated. Dramatic change of the absorption spectrum induced by  $\text{CN}^-$  was observed, while almost no changes could be found in presence of other anions, including  $\text{F}^-$ ,  $\text{Cl}^-$ ,  $\text{Br}^-$ ,  $\text{I}^-$ ,  $\text{AcO}^-$ ,  $\text{HSO}_4^-$ ,  $\text{H}_2\text{PO}_4^-$ ,  $\text{NO}_3^-$ ,  $\text{ClO}_4^-$  (Fig. 9a). More importantly, the color change from pink to colorless can be clearly observed by the naked eye in presence of  $\text{CN}^-$ , while other anions did not induce any significant color change, which suggested that naked-eye selective detection of  $\text{CN}^-$  became possible (Fig. 9b).

Meanwhile, only  $\text{CN}^-$  renders a remarkable “Turn-Off” fluorescence response, whereas all other anions reveal a negligible change in the fluorescent spectra of **DPP2** (Fig. 10a). In the presence of 52 equivalents of  $\text{CN}^-$ , an emission peak at 632 nm with

94.6% fluorescence quenching is observed. Fig. 10b showed the photographs of **DPP2** in the presence of different anions under excitation at 365 nm using a portable UV lamp. The disappearance of intense red color of the solution upon interaction of **DPP2** with  $\text{CN}^-$  is present. However, other anions do not induce any significant emission color change.

Another important feature of **DPP2** is its high selectivity toward the  $\text{CN}^-$  in presence of other competitive anions. Changes of fluorescence response of **DPP2** (10  $\mu\text{M}$ ) caused by  $\text{CN}^-$  (52 equiv) and miscellaneous competing species (52 equiv) were recorded in Fig. S22 (Supporting Information). As can be seen, these competitive species, did not lead to any significant interference. In the presence of these ions, the  $\text{CN}^-$  still produced similar optical spectral changes. These results showed that the selectivity of **DPP2** toward  $\text{CN}^-$  was not affected by the presence of other anions.

Fig. S23 (Supporting Information) showed the time-dependent absorbance at 525 nm of **DPP2** in the presence of  $\text{CN}^-$  (24 equiv.) at room temperature in THF. Generally, reaction-based probes suffer from a long response time. In our case, the response of **DPP2** to  $\text{CN}^-$  is found to be fast. The absorption peak of **DPP2** at 525 nm gradually decreased when 24 equiv. of  $\text{CN}^-$  is added with time passing. After 15 minutes the UV-Vis spectra of **DPP2** are unchangeable, indicating nucleophilic addition reaction between the vinyl group and  $\text{CN}^-$  is completed, which is impressive as many reported cyanide probes require high equivalents of cyanide and long reaction time to reach a maximal spectral signal.<sup>22-31</sup>

### 3.5 Practical application

Active materials-based test strips represent a group of convenient probing substrate for practical utilization. **DPP2**-based test strip was thus fabricated by immersing filter paper into the THF solution of **DPP2** ( $1.0 \times 10^{-3}$  M) and drying in air, which was energy- and cost-effective. The corresponding probing experiments were carried out subsequently. The results indicated that this protocol really took effect. The obvious color change from pink to colorless was observed by immersing this test strips in solutions of  $\text{CN}^-$ , exhibiting colorimetric changes differentiable to naked eyes (Fig. 11a). As shown in Fig. 11b, when the **DPP2**-exposed test strip was immersed into solutions of  $\text{CN}^-$  (0.001 M), strong red fluorescence disappeared and easily distinguished.

### Conclusions

In summary, we described synthesis of two new TPE substituted DPP derivatives (**DPP1** and **DPP2**) and studied comparative fluorescence behaviors. Typically, **DPP1** in dilute THF solution shows the characteristic PL features ( $\lambda_{\text{em}} = 606$  nm) with  $\Phi_f = 32\%$ . Its powder sample emits red fluorescence ( $\lambda_{\text{em}} = 650$  nm,  $\Phi_f = 13\%$ ). **DPP2** in dilute THF solution has  $\Phi_f = 11\%$  ( $\lambda_{\text{em}} = 632$  nm) and its powder sample emits red PL ( $\lambda_{\text{em}} = 615$  nm,  $\Phi_f = 7\%$ ). Moreover, **DPP2** displays high selectivity and sensitivity toward  $\text{CN}^-$ . The strong red emission of **DPP2** was completely quenched in the presence of  $\text{CN}^-$ . However, other anions did not induce any significant change. Test strips for use in practical applications are successfully realized.

### Acknowledgements

The supports by National Basic Research Program of China (2012CB720801), National Natural Science Foundation of China (No. 21274045), the Fundamental Research Funds for the Central Universities (2015ZZ037) and the Natural Science Foundation of Guangdong Province (2015A030313209, 2016A030311034) are gratefully acknowledged.

## References

- 1 (a) L. Deng, W. Wu, H. Guo, J. Zhao, S. Ji, X. Zhang, X. Yuan and C. Zhang, *J. Org. Chem.*, 2011, **76**, 9294; (b) G. Zhang, H. Li, S. Bi, L. Song, Y. Lu, L. Zhang, J. Yu and L. Wang, *Analyst.*, 2013, **138**, 6163; (c) S. Lin, S. Liu, F. Ye, L. Xu, W. Zeng, L. Wang, L. Li, R. Beuerman and D. Cao, *Sensor Actuat B-Chem.*, 2013, **182**, 176; (d) M. V. Ramakrishnam Raju and H. Lin, *Org. Lett.*, 2013, **15**, 13274.
- 2 (a) X. Li, X. Zhang, S. Ghosh and F. Würthner, *Chem. Eur. J.*, 2008, **14**, 8074; (b) Y. Che, X. Yang, K. Balakrishnan, J. Zuo and L. Zang, *Chem. Mater.*, 2009, **21**, 2930; (c) Q. Zhao, K. Li, S. Chen, A. Qin, D. Ding, S. Zhang, Y. Liu, B. Liu, J. Z. Sun and B. Z. Tang, *J. Mater. Chem.*, 2012, **22**, 15128.
- 3 (a) B. Wang, N. He, B. Li, S. Jiang, Y. Qu, S. Qu and J. Hua, *Aust. J. Chem.*, 2012, **65**, 387; (b) Y. Gao, G. Feng, T. Jiang, C. Goh, L. Ng, B. Liu, B. Li, L. Yang, J. Hua, and H. Tian, *Adv. Funct. Mater.*, 2015, **25**, 2857.
- 4 (a) Y. Jin, Y. Xu, Y. Liu, L. Wang, H. Jiang, X. Li and D. Cao, *Dyes Pigments.*, 2011, **90**, 311; (b) L. Wang, L. Yang and D. Cao, *Sensor Actuat B-Chem.*, 2015, **221**, 155.
- 5 (a) Y. Dong, J. W. Y. Lam, A. Qin, J. Liu, Z. Li, B. Z. Tang, J. Sun and H. S. Kwok, *Appl. Phys. Lett.*, 2007, **91**, 11111; (b) Z. Zhao, J. W. Y. Lam and B. Z. Tang, *J. Mater. Chem.*, 2012, **22**, 23726.
- 6 (a) Q. Zhao, S. Zhang, Y. Liu, J. Mei, S. Chen, P. Lu, A. Qin, Y. Ma, J. Z. Sun and B. Z. Tang, *J. Mater. Chem.*, 2012, **22**, 7387; (b) Z. Zhao, S. Chen, J. W. Y. Lam, P. Lu, Y. Zhong, K. S. Wong, H. S. Kwok and B. Z. Tang, *Chem. Commun.*, 2010, 46, **2221**; (c) W. Z. Yuan, P. Lu, S. Chen, J. W. Y. Lam, Z. Wang, Y. Liu, H. S. Kowk, Y. Ma and B.

- Z. Tang, *Adv. Mater.*, 2010, **22**, 2159.
- 7 X. Y. Shen, Y. J. Wang, H. Zhang, A. Qin, J. Z. Sun and B. Z. Tang, *Chem. Commun.*, 2014, **50**, 8747.
- 8 Y. Hong, J. W. Y. Lam and B. Z. Tong, *Chem. Commun.*, 2009, **29**, 4332.
- 9 (a) L. L. Zhu and Y. L. Zhao, *J. Mater. Chem. C*, 2013, **1**, 1059; (b) M. A. Reed, C. Zhou, C. J. Muller, T. P. Burgin and J. M. Tour, *Science*, 1997, **278**, 252; (c) F. Anariba and R. L. McCreery, *J. Phys. Chem. B*, 2002, **106**, 10355; (d) F. Anariba, J. K. Steach and R. L. McCreery, *J. Phys. Chem. B*, 2005, **109**, 11163.
- 10 X. Duan, J. Zeng, J. Lu and Z. Zhang, *J. Org. Chem.*, 2006, **71**, 9873.
- 11 A. Qin, Y. Zhang, N. Han, J. Mei, J. Sun, W. Fan and B. Z. Tong, *Sci. China. Chem.*, 2012, **55**, 772.
- 12 D. Jana, S. Boxi and B. K. Ghorai, *Dyes Pigments.*, 2013, **99**, 740.
- 13 B. Z. Tang, Y. Geng, J. W. Y. Lam, B. Li, X. Jing, X. Wang, F. Wang, A. B. Pakhomov and X. X. Zhang, *Chem. Mater.*, 1999, **11**, 1581.
- 14 (a) X. Y. Shen, Y. J. Wang, E. Zhao, W. Z. Yuan, Y. Liu, P. Lu, A. Qin, Y. Ma, J. Z. Sun and B. Z. Tang, *J. Phys. Chem. C*, 2013, **117**, 7334; (b) W. Z. Yuan, Y. Gong, S. Chen, X. Y. Shen, J. W. Y. Lam, P. Lu, Y. Lu, Z. Wang, R. Hu, Ni. Xie, H. S. Kwok, Y. Zhang, J. Z. Sun and B. Z. Tang, *Chem. Mater.*, 2012, **24**, 1518.
- 15 (a) S. Yoon, J. W. Chung, J. Gierschner, K. S. Kim, M. Choi, D. Kim and S. Y. Park, *J. Am. Chem. Soc.*, 2010, **132**, 13675; (b) S. Yoon and S. Y. Park, *J. Mater. Chem.*, 2011, **21**, 8338.
- 16 C. Shi, Z. Guo, Y. Yan, S. Zhu, Y. Xie, Y. S. Zhao, W. Zhu and He Tian, *ACS. Appl.*

*Mater. Interfaces*, 2013, **5**, 192.

17 (a) J. Jiang, X. Wang, W. Zhou, H. Gao and J. Wu, *Phys. Chem. Chem. Phys.*, 2002, **4**, 4489; Z. Xu, X. Chen, H. N. Kim and J. Yoon, *Chem. Soc. Rev.*, 2010, **39**, 127.

18 (a) Y. D. Lin, Y. S. Pen, W. T. Su, K. L. Liao, Y. S. Wen, C. H. Tu, C. H. Sun, T. J. Chow, *Chem-Asian J.*, 2012, **7**, 2864; (b) Y. M. Dong, Y. Peng, M. Dong, Y. M. Wang, *J. Org. Chem.*, 2011, **76**, 6962; (c) M. Dong, Y. Peng, Y. M. Dong, N. Tang, Y. W. Wang, *Org. Lett.*, 2012, **14**, 130; (d) Z. P. Liu, X. Q. Wang, Z. H. Yang, W. J. He, *J. Org. Chem.*, 2011, **76**, 10286; (e) S. Khatua, D. Samanta, J. W. Bats, M. Schmittel, *Inorg. Chem.*, 2012, **51**, 7075; (f) L. Yuan, W. Y. Lin, Y. T. Yang, J. Z. Song, J. L. Wang, *Org. Lett.*, 2011, **13**, 3730; (g) X. H. Huang, X. G. Gu, G. X. Zhang, D. Q. Zhang, *Chem. Commun.*, 2012, **48**, 12195; (h) J. T. Zhang, S. L. Zhu, L. Valenzano, F. T. Luo, H. Y. Liu, *RSC Adv.*, 2010, **3**, 68; (i) S. Park, H. J. Kim, *Chem. Commun.*, 2010, **46**, 9197; (j) C. R. Maldonado, A. Touceda-Varela, A. C. Jones, J. C. Mareque-Rivas, *Chem. Commun.*, 2011, **47**, 11700; (k) T. W. Hudnall, F. P. Gabbaï, *J. Am. Chem. Soc.*, 2007, **129**, 11978; (l) T. Gomez, D. Moreno, Greñu B. Díazde, A. C. Fernández, T. Rodríguez, J. Rojo, J. V. Cuevas, T. Torroba, *Chem-Asian J.*, 2013, **8**, 1271; (m) Y. D. Lin, Y. S. Peng, W. T. Su, C. H. Tu, C. H. Sun, T. J. Chow, *Tetrahedron* 2012, **68**, 2523; (n) T. F. Robbins, H. Qian, H. Su, R. P. Hughes, I. Aprahamian, *Org. Lett.*, 2013, **15**, 2386; (o) Q. Lin, X. Liu, T. B. Wei, Y. M. Zhang, *Chem-Asian J.*, 2013, **8**, 3015; (p) X. S. Zhou, X. Lv, J. S. Hao, D. S. Liu, W. Guo, *Dyes Pigm.*, 2012, **95**, 168; (q) M. Tomasulo, F. M. Raymo, *Org. Lett.*, 2005, **7**, 4633; (r) M. Tomasulo, S. Sortino, A. J. P. White, F. M. Raymo, *J. Org. Chem.*, 2006, **71**,

- 744; (s) Yang YK, Tae J *Org. Lett.*, 2006, **8**, 5721; (t) Y. T. Yang, C. X. Yin, F. J. Huo, J. B. Chao, Y. B. Zhang, F. Q. Cheng, *Sensors and Actuators B, Chem.*, 2014, **193**, 220; (u) J. Huo, J. Su, Y. Q. Sun, C. X. Yin, J. B. Chao, *Chem. Lett.*, 2010, **39**, 2738; (v) F. J. Huo, J. Kang, C. X. Yin, J. B. Chao, Y. B. Zhang, *Sensors and Actuators B, Chem.*, 2015, **215**, 93; (w) Y. K. Yue, F. J. Huo, C. X. Yin, J. B. Chao, Y. B. Zhang. *Sensors and Actuators B, Chem.*, 2015, **212**, 451.
- 19 (a) L. Wang, J. Du and D. Cao, *Sensor Actuat B-Chem.*, 2014, **205**, 281; (b) L. Wang, L. Zhu and D. Cao, *New J. Chem.*, 2015, **39**, 7211.
- 20 *Guidelines for Drinking-Water Quality*, 3rd ed.; World Health Organization: Geneva, 2004.
- 21 (a) B. Shi, P. Zhang, T. Wei, H. Yao, Q. Lin and Y. Zhang, *Chem. Commun.*, 2013, **49**, 7812; (b) L. G. Nandi, C. R. Nicoletti, I. C. Bellettini and V. G. Machado, *Anal. Chem.*, 2014, **86**, 4653; (c) X. Lou, D. Ou, Q. Li and Z. Li, *Chem. Commun.*, 2012, **48**, 8462.
- 22 C. Chow, M. H. W. Lam and W. Y. Wong, *Inorg. Chem.*, 2004, **43**, 8387.
- 23 J. H. Lee, A. R. Jeong, I. Shin, H. Kim and J. Hong, *Org. Lett.*, 2010, **12**, 764.
- 24 H. N. Kim, Z. Guo, W. Zhu, J. Yoon and H. Tian, *Chem. Soc. Rev.*, 2011, **40**, 79.
- 25 X. Lou, L. Zhang, J. Qin and Z. Li, *Chem. Commun.*, 2008, 5848.
- 26 X. Lou, J. Qin and Z. Li, *Analyst*, 2009, **134**, 2071.
- 27 Q. Zeng, P. Cai, Z. Li, J. Qin and B. Z. Tang, *Chem. Commun.*, 2008, 1094.
- 28 X. Lou, L. Qiang, J. Qin and Z. Li, *ACS Appl. Mater. Interfaces*, 2009, **1**, 2529.
- 29 H. Yu, Q. Zhao, Z. Jiang, J. Qin and Z. Li, *Sensor Actuat. B-Chem.*, 2010, **148**,

110.

30 M. Jamkratoke, V. Ruangpornvisuti, G. Tumcharern, T. Tuntulani, and B.

Tomapatanaget, *J. Org. Chem.*, 2009, **74**, 3919.

31 J. V. Ros-Lis, R. Martinez-Manez, and J. Soto, *Chem. Commun.*, 2005, 5260.

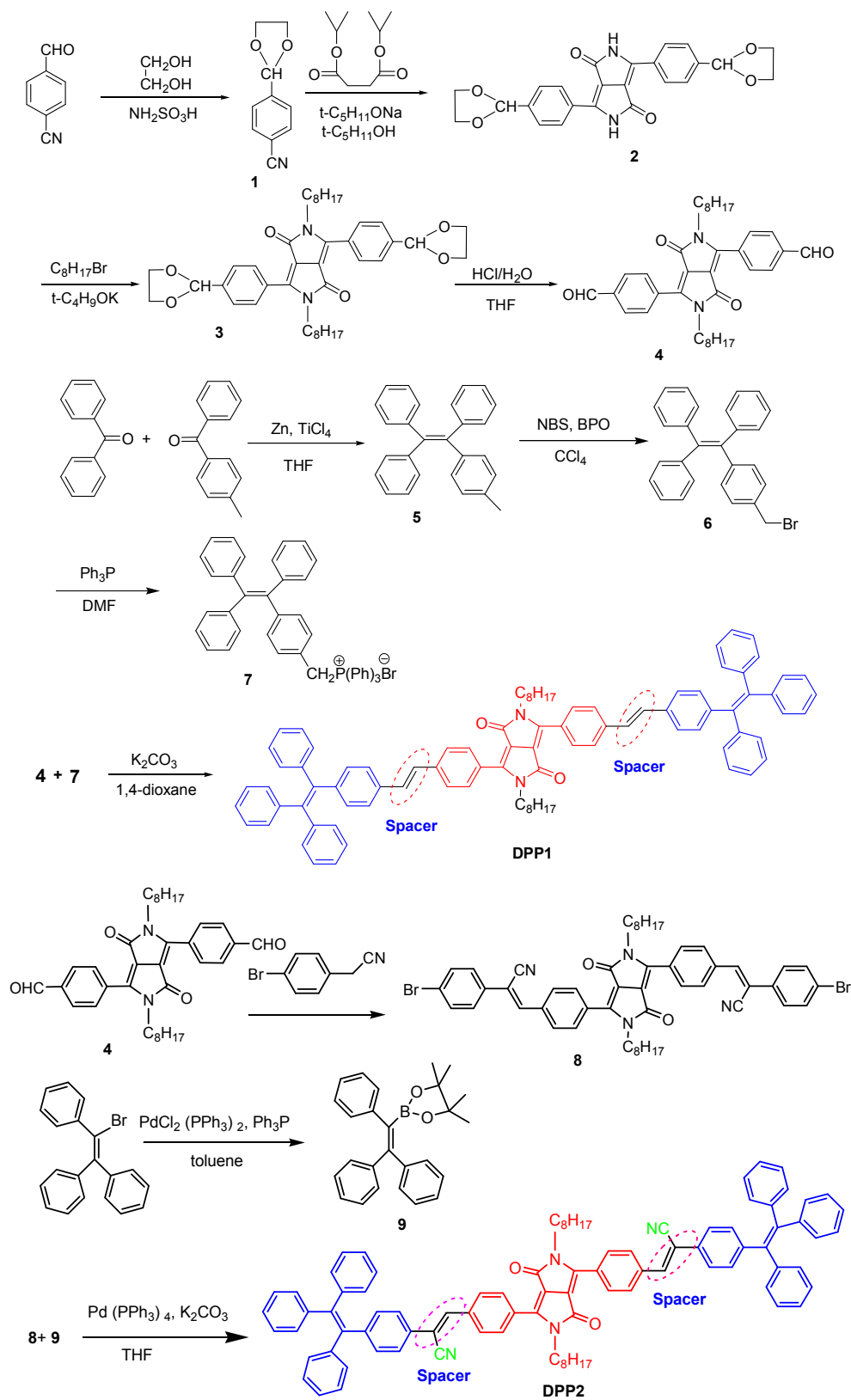
Scheme 1. Synthesis of **DPP1** and **DPP2**.

Table 1. Photophysical data of **DPP1** and **DPP2** in solution and solid state.

	THF <sup>a</sup>						Solid-state	
	HOMO (ev)	LUMO (ev)	gap (ev)	$\lambda_{ab}$ (nm)	$\lambda_{em}$ (nm)	$\Phi_f$ <sup>b</sup>	$\lambda_{em}$ (nm)	$\Phi_f$ <sup>c</sup>
<b>DPP1</b>	-5.17	-1.69	3.48	513	605	32%	650	13%
<b>DPP2</b>	-5.38	-2.21	3.17	526	632	11%	615	7%

<sup>a</sup> Measured at a concentration of 10  $\mu$ M at 25  $^{\circ}$ C; <sup>b</sup> estimated using Rhodamine 6G ( $\Phi_f$ =95% in ethanol) as reference; <sup>c</sup> Absolute quantum yield determined by calibrated integrating sphere systems.

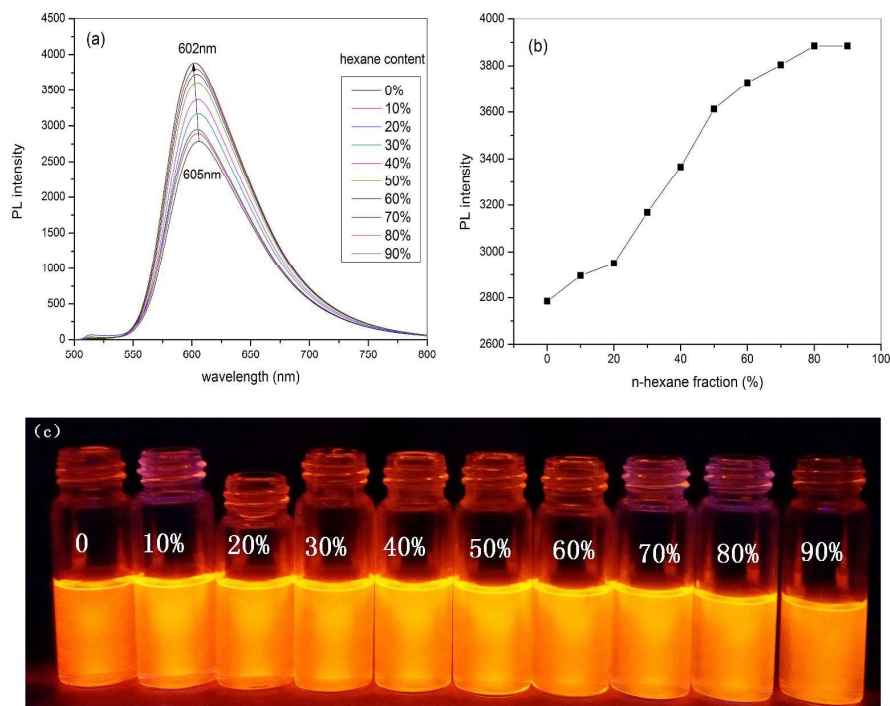


Fig.1 (a) The photoluminescence (PL) spectra, (b) PL intensity vs  $f_h$  and (c) emission photographs of **DPP1** in CHCl<sub>3</sub>/hexane mixtures with different  $f_h$  values.

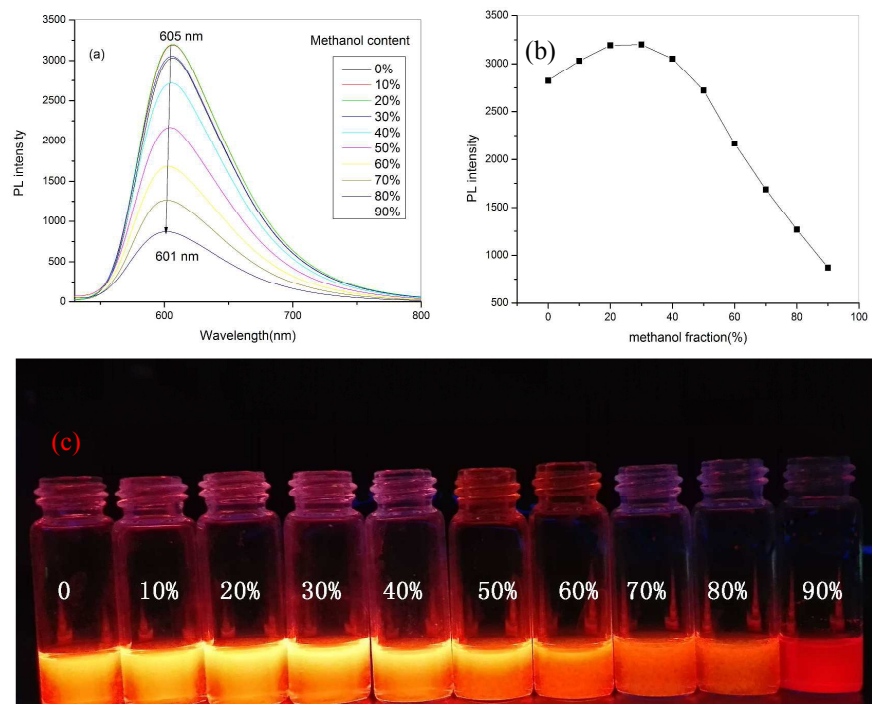


Fig.2 (a) The photoluminescence (PL) spectra, (b) PL intensity vs  $f_m$  and (c) emission photographs of **DPP1** in  $\text{CHCl}_3$ /methanol mixtures with different  $f_m$  values.

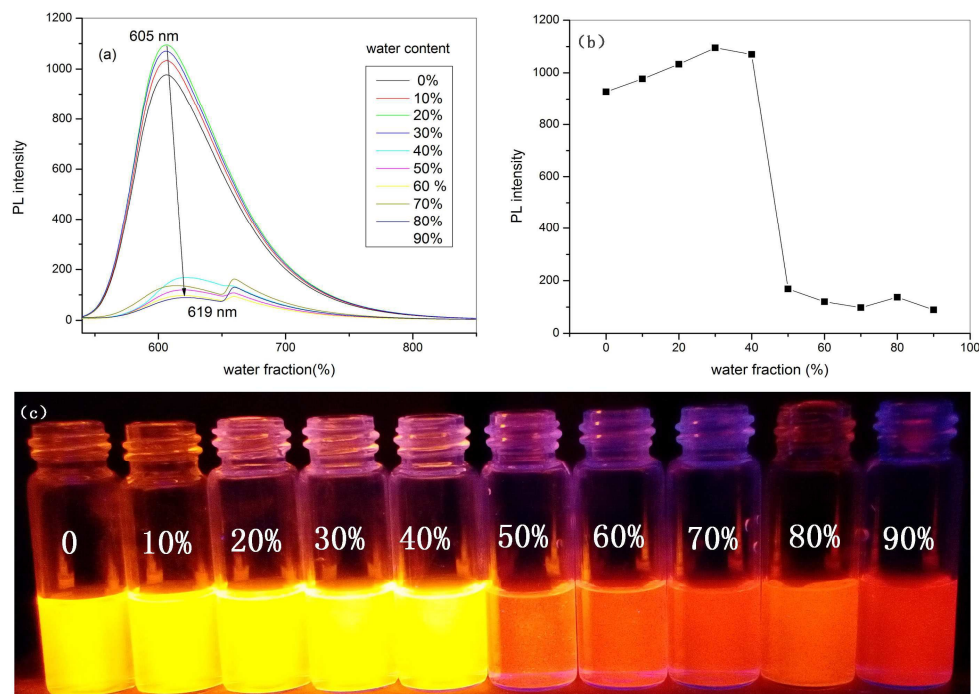


Fig.3 (a) The photoluminescence (PL) spectra, (b) PL intensity vs  $f_w$  and (c) emission photographs of **DPP1** in THF/water mixtures with different  $f_w$  values.

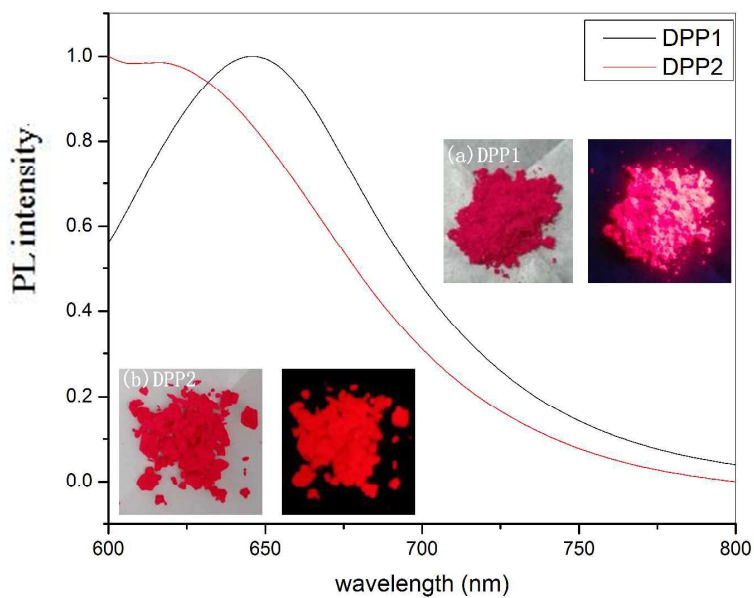


Fig.4 Normalized photoluminescence (PL) spectra of **DPP1** and **DPP2** in powder.

Inset: color and emission photographs of **DPP1** and **DPP2**.

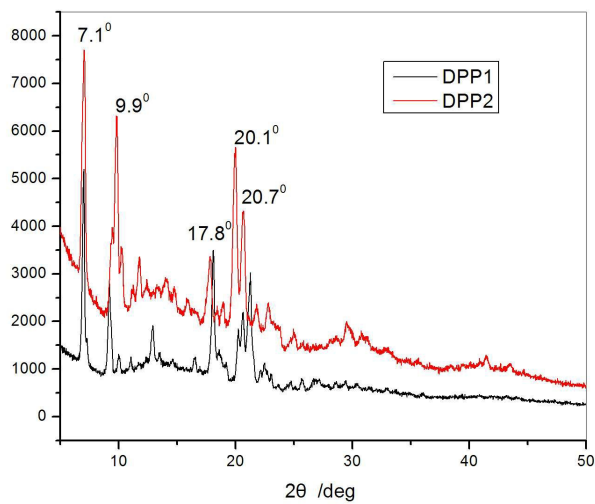


Fig. 5 XRD patterns of **DPP1** and **DPP2** in solid powder.

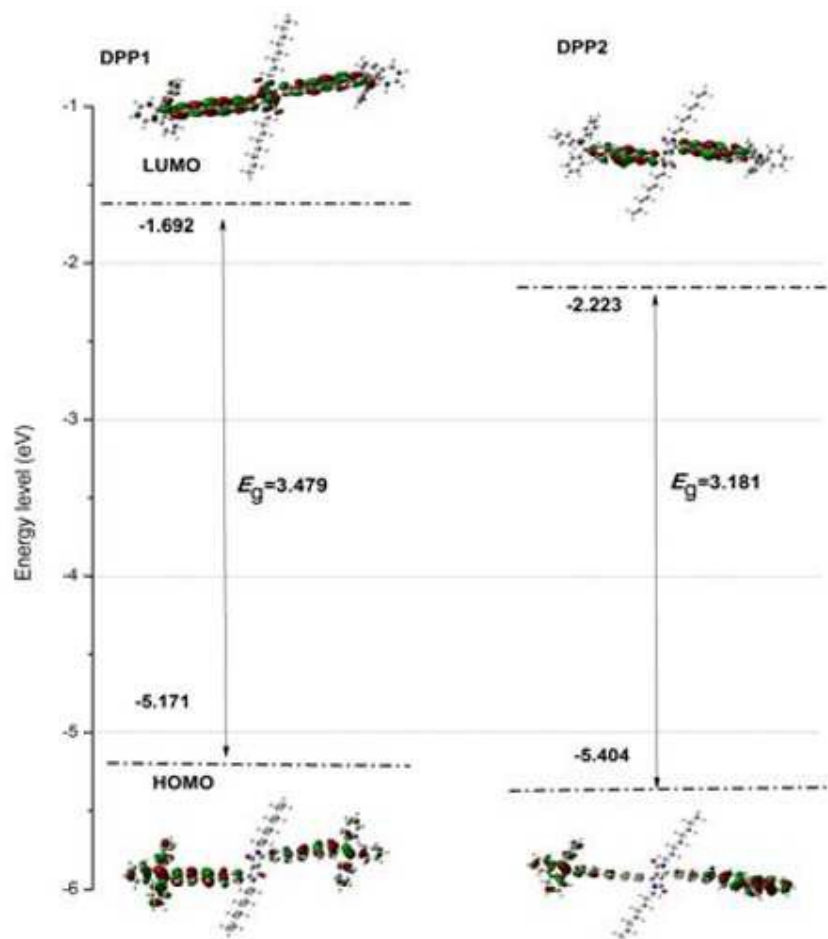


Fig. 6 Energy level alignment and electron distribution of **DPP1** and **DPP2**.

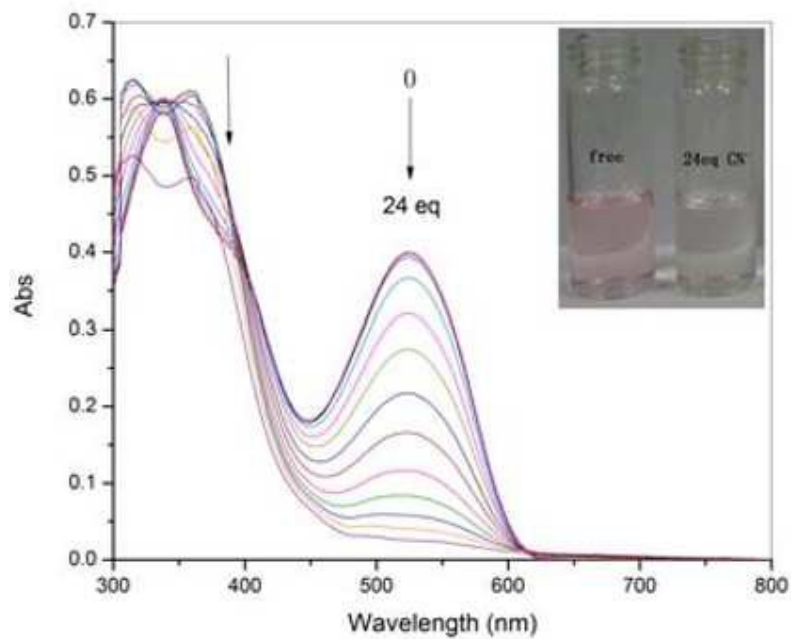


Fig. 7 UV-Vis spectral changes of **DPP2** in THF (10 μM) with the increasing concentrations of cyanide anion.

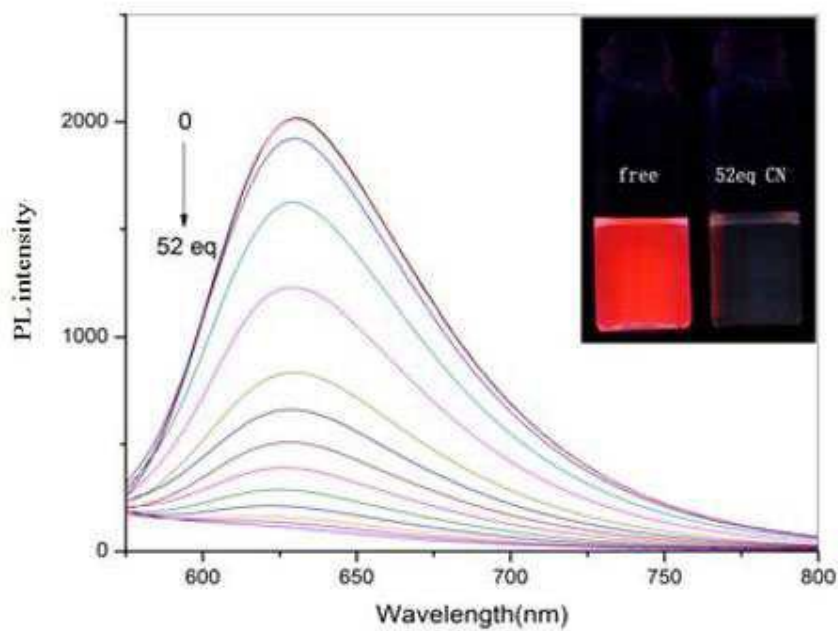


Fig. 8 The photoluminescence (PL) spectral changes of **DPP2** (10 μM) in THF with the increasing concentrations of CN<sup>-</sup> in THF under excitation at 520 nm.

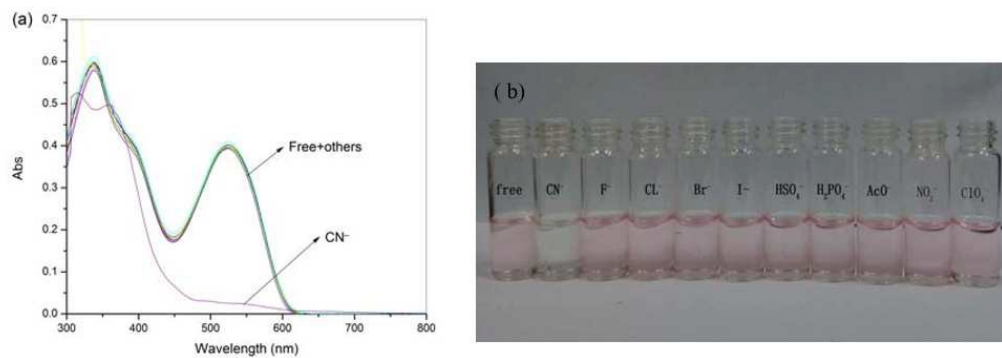


Fig. 9 (a) UV-vis absorption spectra and (b) color changes of **DPP2** in THF (10 μM) upon addition of 24 equiv. of each anion.

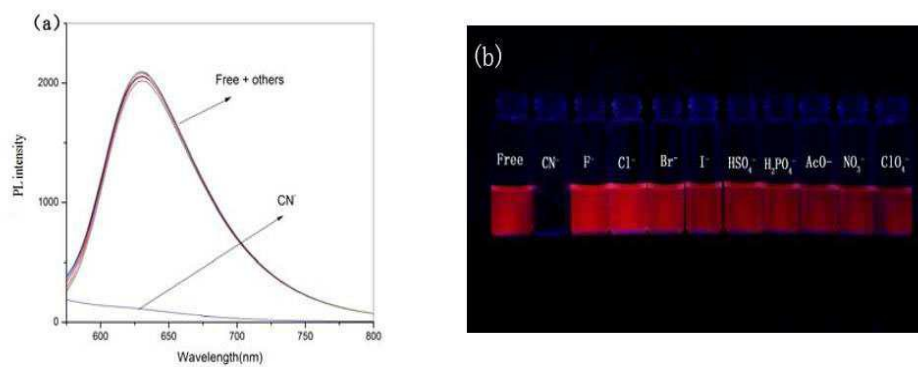


Fig. 10 (a) Photoluminescence (PL) and (b) emission color changes of **DPP2** in THF (10  $\mu$ M) upon addition of 52 equiv. of each anion aqueous solution.

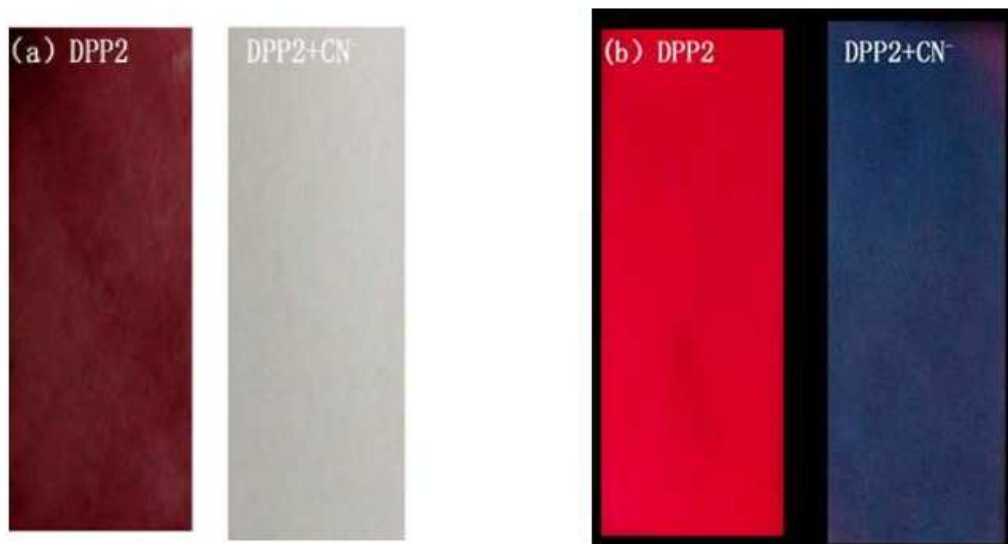
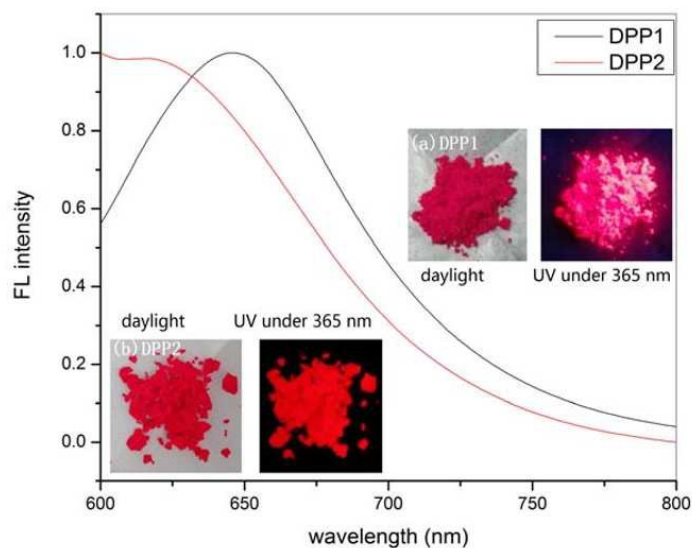
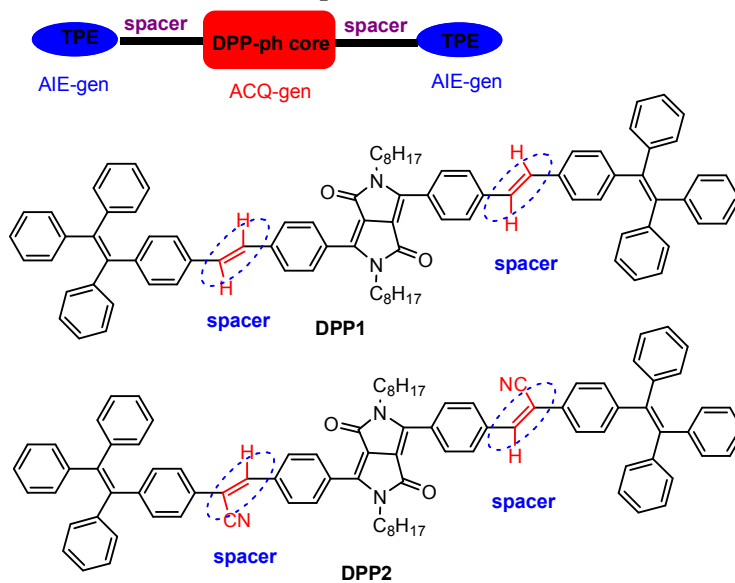


Fig. 11 (a) Color and (b) emission changes of **DPP2**-based test strips before and after addition of  $\text{CN}^-$ .

## Graphic abstract



Tetraphenylethene -functionalized diketopyrrolopyrrole solid state red-emissive molecules (**DPP1** and **DPP2**) with enhanced emission in the solid state have been developed.